

# Near-infrared absorption and semimetal-semiconductor transition in 2 nm ErAs nanoparticles embedded in GaAs and AlAs

Michael A. Scarpulla,<sup>1,a)</sup> Joshua M. O. Zide,<sup>1</sup> James M. LeBeau,<sup>1</sup>  
Chris G. Van de Walle,<sup>1</sup> Arthur C. Gossard,<sup>1</sup> and Kris T. Delaney<sup>2</sup>

<sup>1</sup>Materials Department, University of California, Santa Barbara, California 93106-5050, USA

<sup>2</sup>Materials Research Laboratory, University of California, Santa Barbara, California 93106-5121, USA

(Received 27 February 2008; accepted 21 March 2008; published online 1 May 2008)

We report strong near-infrared absorption peaks in epitaxial films of GaAs and AlAs containing approximately 0.5–5% of the semimetal ErAs. The energy of the resonant absorption peak can be changed from 0.62 to 1.0 eV (2.2–1.4  $\mu\text{m}$ ) by variation of the ErAs volume fraction and the substrate temperature. We interpret the infrared absorption in terms of transitions across an energy gap caused by a confinement-induced semimetal-semiconductor transition. An effective mass model relates the changes in nanoparticle diameter observed in transmission electron microscopy to the energy gap. © 2008 American Institute of Physics. [DOI: 10.1063/1.2908213]

Strong near-infrared absorption peaks have been measured in films of GaAs and GaSb containing nanoislands of the semimetals ErAs or ErSb with approximate dimensions of 1.5 nm  $\times$  10 nm  $\times$  20 nm.<sup>1,2</sup> This absorption was interpreted as surface plasmon resonances (SPRs) assuming that the ErAs islands were bulk-like. Herein, we investigate absorption from  $\sim$ 2 nm diameter nearly spherical ErAs nanoparticles embedded in GaAs or AlAs. We find a similar absorption feature that can be manipulated both in magnitude and peak energy by variation of molecular beam epitaxy (MBE) growth parameters.

In this letter, we propose that the absorption from 2 nm diameter ErAs nanoparticles is consistent with quantum size effects within an effective mass model. The calculated confinement energies are sufficient to lift the semimetallic band overlap in the ErAs nanoparticles for diameters below  $\sim$ 3 nm, leading to a semiconductor-like energy level arrangement. Previously, evidence for a confinement-induced semimetal-semiconductor transition has been found in studies of Bi nanowires and HgTe nanoparticles.<sup>3,4</sup>

In bulk ErAs, the valence band maximum is at  $\Gamma$  and the conduction band minimum is at  $X$  resulting in  $(2-3) \times 10^{20} \text{ cm}^{-3}$  electrons and holes.<sup>5</sup> Rocksalt ErAs has  $a = 5.74 \text{ \AA}$  resulting in 1.6% lattice mismatch to GaAs and 1.4% to AlAs.<sup>6,7</sup> When (In,Ga)As or GaAs and 0.1%–6% ErAs are codeposited by MBE,  $\sim$ 2 nm diameter ErAs nanoparticles form.<sup>8,9</sup> These embedded self-assembled nanoparticles are exemplary for investigating semimetallic nanostructures because of their small size and epitaxial interfaces.

Samples were grown on semi-insulating (001) GaAs in a solid-source MBE system. The 200–1000 nm nanoparticle-containing layers were grown by simultaneously depositing ErAs and GaAs (AlAs) and were capped with 100 nm of GaAs at 600 °C. Film compositions were determined from ErAs, GaAs, and AlAs film growth rates. Absorption data were measured using a spectrophotometer and the absorption coefficient was approximated as  $-\ln(T/T_0)/t$ , where  $T$  is the measured sample transmission,  $T_0$  is the transmission of a GaAs substrate, and  $t$  is the ErAs-containing layer thickness. A FEI T20 transmission electron microscope (TEM) with

$C_s \sim 2.0 \text{ mm}$  operated at 200 kV was used for high-resolution imaging of the particles.

Absorption data from a series of GaAs samples with ErAs volume fractions of 0.7%, 2.0%, 3.2%, and 4.5% are shown in Fig. 1. The magnitude of the peak increases linearly with increasing ErAs volume fraction, suggesting an increase in the number of absorbers. This is consistent with TEM measurements showing that the ErAs nanoparticle density increases over the composition range 0.3%–6% ErAs. We interpret the width of the absorption peak as a result from the nanoparticle size distribution. The shifting of the absorption peak with composition is under further investigation but may be caused by wavefunction hybridization between nanoparticles as their mean center-to-center spacing decreases from  $\sim$ 8.4 to 4.5 nm from 0.7 to 4.5% ErAs.

Figure 2(a) presents the absorption from a separate series of GaAs films with 3.2% ErAs grown at substrate temperatures from 500–600 °C. The peak energy redshifts 61% from 998 to 618 meV over this range of temperatures. Figure 2(b) presents data from AlAs films containing 3.2% ErAs and shows a weaker temperature dependence. In our films containing  $\sim$ 3% ErAs in GaAs, TEM demonstrates that the average diameter increases with deposition temperature and

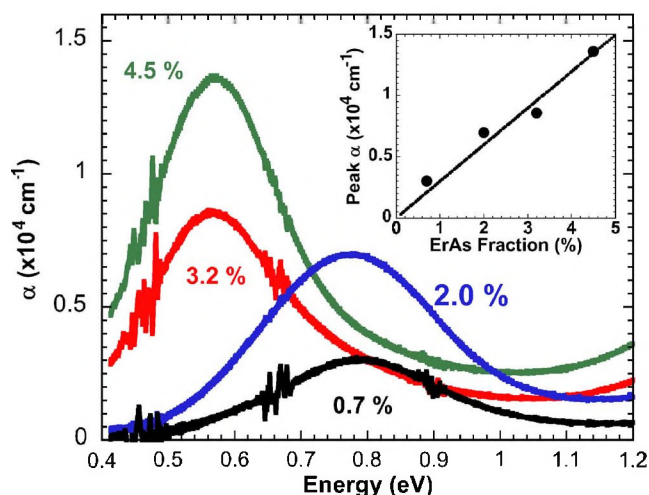


FIG. 1. (Color online) (Main) Absorption data for GaAs-ErAs grown at 600 °C vs ErAs volume fraction. (Inset) Peak absorption coefficient vs ErAs volume fraction with best-fit linear trendline.

<sup>a)</sup>Electronic mail: mikes@engr.ucsb.edu.

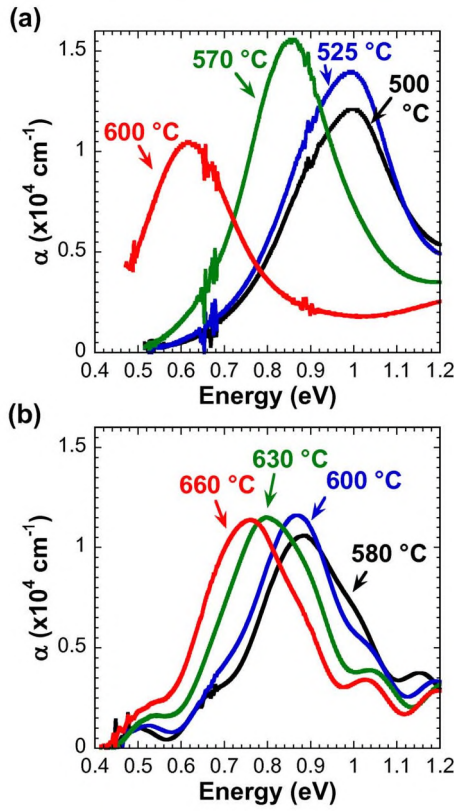


FIG. 2. (Color online) Absorption data for 3.2% ErAs in (a) GaAs and (b) AlAs for different deposition temperatures. The data for AlAs–ErAs layers exhibit Fabry–Perot oscillations.

is 1.7, 1.8, and 2.0 nm for films grown at 540, 570, and 600 °C, respectively. This suggests that the shift in absorption peak energy may be related to the change in physical size of the nanoparticles.

Quantum confinement in the ErAs nanoparticles resulting in the opening of an energy gap can account for the strong variation of the absorption peak with nanoparticle size. We assume that the confinement potentials for electrons and holes are provided by the energy difference of the band extrema in GaAs and ErAs, as depicted in Fig. 3(a). For example, the barrier for holes is given by the GaAs bandgap minus the  $n$ -type Schottky barrier height for ErAs on GaAs plus half of the ErAs  $\Gamma$ - $X$  overlap. The Schottky barrier height for ErAs on  $n$ -GaAs varies with crystalline orientation;<sup>10</sup> spherical averaging yields a value of  $\sim 0.75$  eV. Using  $G_0W_0$  quasiparticle-energy calculations, we calculate the  $\Gamma$ - $X$  overlap in bulk ErAs to be  $\sim 0.7 \pm 0.1$  eV with  $E_F$  being close to midway between the band extrema.<sup>11</sup> We consider the possibilities that the electron confinement is provided by the GaAs  $\Gamma$  or  $X$  band minima. The confinement potential is 1.12 eV for holes and is 1.10 eV (1.56 eV) for the electron  $\Gamma$  ( $X$ ) case.

We model the nanoparticles with a spherical finite-step potential  $V(r) = -V_0$  for radius  $r < a$  and  $V(r) = 0$  for  $r \geq a$ .<sup>12</sup> The ground state energies are found from

$$\left. \frac{1}{m_{\text{in}}^*} \frac{\partial}{\partial r} \ln(\psi_{\text{in}}) \right|_{r=a} = \left. \frac{1}{m_{\text{out}}^*} \frac{\partial}{\partial r} \ln(\psi_{\text{out}}) \right|_{r=a}, \quad (1)$$

We use the heavy hole masses  $m_{\text{hh}}^*/m_0 = 0.5$  (0.76) for GaAs (AlAs). For ErAs, our  $G_0W_0$  calculation yields  $m_{\text{hh}}^*/m_0 = 0.235$  at  $\Gamma$ . The  $G_0W_0$  calculations give  $m_{\text{hh}}^*/m_0 = 0.176$

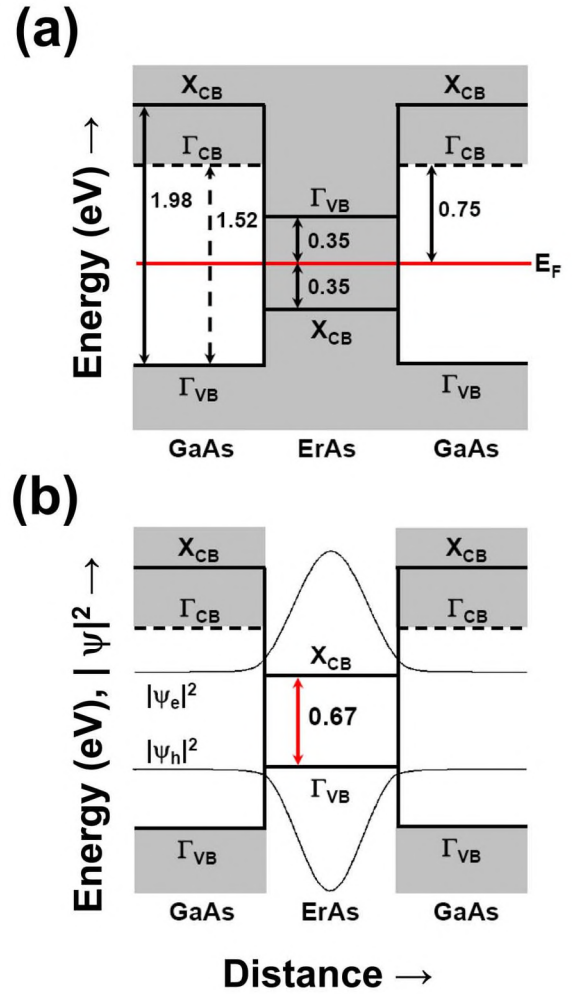


FIG. 3. (Color online) Schematic band diagrams (a) before and (b) after accounting for quantum confinement in a 2 nm nanoparticle assuming the GaAs  $X$  barrier. Regions with continuous density of states are shaded.

and  $m_{e,\parallel}^*/m_0 = 1.289$  for the band-edge  $X$  electrons in ErAs, and we use  $m_{e,\perp}^*/m_0 = 0.23$  (0.22) and  $m_{e,\parallel}^*/m_0 = 1.3$  (0.97) for GaAs (AlAs).<sup>13</sup> Spherically averaging the principle axes of the  $X$  pocket using

$$m_{e,X}^* = \frac{3m_{e,\perp}m_{e,\parallel}}{2m_{e,\parallel} + m_{e,\perp}} \quad (2)$$

results in  $m_{e,X}^*/m_0 = 0.25$ , 0.32, and 0.30 for ErAs, GaAs, and AlAs, respectively. For GaAs,  $m_{e,\Gamma}^*$  was taken as  $0.066m_0$ .

For ErAs nanoparticles in GaAs, solving Eq. (1) for both electrons and holes predicts the opening of a bandgap for diameters  $2a$  less than  $\sim 3$  nm. The experimentally observed 1.7–2.0 nm diameter particles are clearly in this regime. For nanoparticles with these diameters, no bound excited states exist for electrons or holes. Figure 3(b) depicts the energy levels and wavefunctions for a 2 nm diameter ErAs nanoparticle embedded in GaAs within the  $X$ -barrier model. Assuming no shift of the Fermi level in the matrix, the ErAs valence state is occupied while the excited state is unoccupied at 0 K. The conduction band minimum in ErAs is composed of Er 5d states, while the valence band maximum is made up of As 4p states; thus, optical transitions between the confined states are dipole-allowed. We assume that the crystal momentum selection rule is relaxed because of the nanopar-



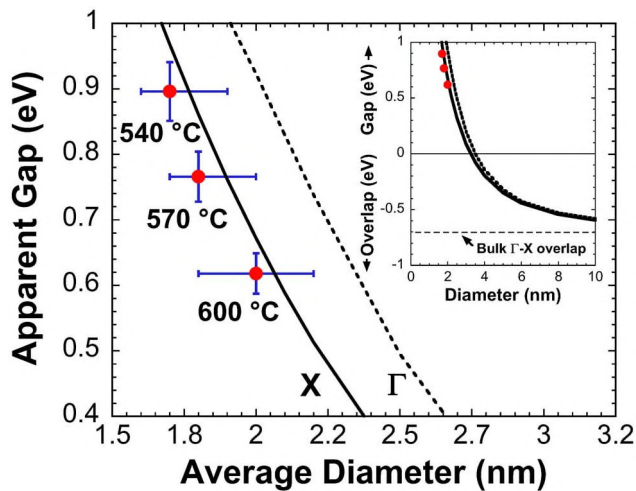


FIG. 4. (Color online) Experimental peak absorption energy vs TEM-determined ErAs nanoparticle size for 3.2% ErAs in GaAs. Predictions of the GaAs X and  $\Gamma$  minima models are shown by solid and dashed lines, respectively.

ticles' extremely small sizes. Thus, we interpret the observed absorption as resulting from transitions across the confinement-induced energy gap.

Figure 4 plots the calculated energy gap for ErAs nanoparticles embedded in GaAs, the experimentally determined absorption peak energies, and the particle sizes from TEM measurements. Despite the lower  $\Gamma$  barrier height, the small GaAs  $m_{e,\Gamma}^*$  pushes the  $\Gamma$  energies higher than those associated with the X barrier. The model assuming that the GaAs X minimum provides the confinement barrier gives better agreement with the available data. An estimate of the exciton correction is given by

$$\frac{1}{4\pi\epsilon_r\epsilon_0} \frac{q^2}{a}, \quad (3)$$

where  $\epsilon_0$  is the vacuum permittivity, the relative permittivity  $\epsilon_r$  is taken as  $\sim 15$  for ErAs, and  $q$  is the electron charge. For a 1.8 nm diameter nanoparticle, Eq. (3) gives 0.11 eV which would bring the model using the GaAs X barrier very close to the experimental data. Size measurements of ErAs nanoparticles in AIs are not available, however, assuming a diameter of 2 nm and applying the X barrier model results in a similar level arrangement and predicted transition energy of 0.55 eV, which is somewhat lower than the peak energies in Fig. 2(b).

Despite the similarities of the absorption features in samples containing ErAs nanoislands (1.5 nm  $\times$  10 nm  $\times$  20 nm) and spherical nanoparticles (2 nm diameter), we believe that the underlying physics are different primarily because of the redshift of the absorption feature with growth temperature. Four mechanisms exist that could redshift a SPR in embedded ErAs nanoparticles.<sup>14</sup> First, decreasing the nanoparticle carrier concentration would redshift such a SPR. However, each  $\sim 4 \times 10^{-21}$  cm<sup>3</sup> ErAs nanoparticle would only contain one electron and one hole were its band-structure bulklike. Second, if increasing growth temperature changed a nanoparticle's aspect ratio, this could cause a redshift and dichroism.<sup>2</sup> However, our TEM studies exclude significant elongation or contraction along the growth direction and we observe no dichroism for light polarized along the in-plane [110] and  $\bar{1}\bar{1}0$  directions. Third, boundary scatter-

ing can change the carrier scattering time and thus SPR energy. Quantitative Drude modeling of the ErAs dielectric constant indicates that the possible change in SPR energy from 1.7 to 2.0 nm diameter particles cannot account for the observed 60% redshift. Lastly, dipole coupling between metallic bodies is known to cause SPR redshifts, however, the redshift of the peak observed for changing the spacing for 4 nm diameter Ag nanoparticles from 5 to 0.5 nm amounted to only  $\sim 2\%$ .<sup>15</sup> Therefore, the existing experimental evidence does not appear consistent with an interpretation in terms of SPRs.

For larger ErAs and ErSb nanoislands,<sup>1,2</sup> the small ( $\sim 1.5$  nm) dimension would cause approximately 0.4 eV confinement energy while contributions from the larger dimensions would be negligible. It has also been reported that layers of ErAs in GaAs as thin as 0.7 nm remain semimetallic.<sup>16</sup> Thus, our interpretation is that such ErAs and ErSb nanoislands remain on the semimetal side of the semimetal-semiconductor transition.

Optical absorption was investigated in layers of GaAs and ErAs with 0.7–4.5 vol % embedded epitaxial ErAs nanoparticles with diameter of  $\sim 2$  nm. The films exhibit a strong absorption feature that can be changed in magnitude and peak energy by variation of the growth temperature and ErAs fraction. An effective mass model of quantum confinement indicates a semimetal-semiconductor transition and the observed absorption is consistent with excitation of electrons across the resulting energy gap.

Support was from NSF MRSEC (DMR05-20415). J.M.L. acknowledges a Dept. of Ed. GAANN fellowship (P200A07044). We thank J. Zimmerman, M. Hanson, P. Petroff, D. Smith, and H. Kroemer for discussions and L. Coldren, D. Cohen, and J. English for assistance.

<sup>1</sup>E. R. Brown, A. Bacher, D. Driscoll, M. Hanson, C. Kadow, and A. C. Gossard, *Phys. Rev. Lett.* **90**, 077403 (2003).

<sup>2</sup>M. P. Hanson, A. C. Gossard, and E. R. Brown, *J. Appl. Phys.* **102**, 043112 (2007).

<sup>3</sup>A. Rogach, S. Kershaw, M. Burt, M. Harrison, A. Kornowski, A. Eychmüller, and H. Weller, *Adv. Mater. (Weinheim, Ger.)* **11**, 552 (1999).

<sup>4</sup>Z. Zhang, X. Sun, M. S. Dresselhaus, J. Y. Ying, and J. P. Heremans, *Appl. Phys. Lett.* **73**, 1589 (1998).

<sup>5</sup>S. J. Allen, N. Tabatabaie, C. J. Palmstrom, G. W. Hull, T. Sands, F. Derosa, H. L. Gilchrist, and K. C. Garrison, *Phys. Rev. Lett.* **62**, 2309 (1989).

<sup>6</sup>D. O. Klenov, J. M. Zide, J. D. Zimmerman, A. C. Gossard, and S. Stemmer, *Appl. Phys. Lett.* **86**, 241901 (2005).

<sup>7</sup>T. Sands, C. J. Palmstrom, P. H. J. V. G. Keramidis, N. Tabatabaie, T. L. Cheeks, R. Ramesh, and Y. Silberberg, *Mater. Sci. Rep.* **5**, 99 (1990).

<sup>8</sup>J. M. Zide, D. O. Klenov, S. Stemmer, A. C. Gossard, G. Zeng, J. E. Bowers, D. Vashaee, and A. Shakouri, *Appl. Phys. Lett.* **87**, 112102 (2005).

<sup>9</sup>D. O. Klenov, J. M. O. Zide, J. M. LeBeau, A. C. Gossard, and S. Stemmer, *Appl. Phys. Lett.* **90**, 121917 (2007).

<sup>10</sup>C. J. Palmstrom, T. L. Cheeks, H. L. Gilchrist, J. G. Zhu, C. B. Carter, B. J. Wilkens, and R. Martin, *J. Vac. Sci. Technol. A* **10**, 1946 (1992).

<sup>11</sup>K. T. Delaney, N. A. Spaldin, and C. G. V. d. Walle (unpublished).

<sup>12</sup>B. H. Bransden and C. J. Joachain, *Quantum Mechanics* (Prentice Hall, Essex, England, 2000).

<sup>13</sup>I. Vurgaftman, J. R. Meyer, and L. R. Ram-Mohan, *J. Appl. Phys.* **89**, 5815 (2001).

<sup>14</sup>C. F. Bohren and D. R. Huffman, *Absorption and Scattering of Light by Small Particles* (Wiley, New York, 1983).

<sup>15</sup>C. P. Collier, R. J. Saykally, J. J. Shiang, S. E. Henrichs, and J. R. Heath, *Science* **277**, 1978 (1997).

<sup>16</sup>S. J. Allen, N. Tabatabaie, C. J. Palmstrom, S. Mounier, G. W. Hull, T. Sands, F. Derosa, H. L. Gilchrist, and K. C. Garrison, *Surf. Sci.* **228**, 13 (1990).